Dynamics of 2-dim Expanding Slow Hydrogen-Air Flames in Cylindrical Horizontal Hele-Shaw Cell

Moskalev P.V.[1)], Filippov A.E.[2)], Nikolaev I.I.[2)], Denisenko V.P.[2)],
Gubernov V.V. [3)], Plaksin V.Yu. [4)], Kirillov I.A. [2)]
[1)] Voronezh State Technical University, Voronezh, Russia
[2)] National Research Centre "Kurchatov Institute", Moscow, Russia
[3)] P.N. Lebedev Physical Institute of the Russian Academy of Sciences, Moscow, Russia
[4)] Kintech Lab Ltd, Moscow, Russia

1 Introduction

Flame speed (laminar or turbulent) is one of the most important characteristics of the premixed combustible mixtures in the academic and applied studies. Normal laminar flame speed $v_L(\phi, T_u, p_u)$ is used as an intrinsic physico-chemical property of a combustible mixture and as a scaling parameter for the turbulent flame speed. Burning or visible velocity v_b of the fast turbulent flames is widely used for assessing mechanical loads of structures subjected to gas explosions.

Propagation characteristics of the flames in hydrogen-containing mixtures have been studied, mainly, in closed vessels or in open spaces for the outward expanding 3-dim spherical flames [1-6]. From the point of view of flame dynamics, the lean hydrogen mixtures are mostly interesting since the onset of flame instabilities may cause the reaction front segmentation and acceleration.

Experimental information on dynamics of the quasi-2-dim expanding flames is much more limited. In [7] the cylindrical expanding quasi-2-dim flames were studied for the ultra-lean (< 10 vol.% H_2) hydrogen-air mixtures under normal initial conditions in horizontal, axisymmetric, closed Hele-Shaw cell. In [8] the spherical and cylindrical flames were studied for lean and near-stoichiometric mixtures between 10 and 45 vol.% H_2 in vertical, rectangular, open Hele-Shaw cell.

Goals of this work – to study systematically the changes in dynamics of the quasi-2-dim cylindrically expanding slow flames with different morphology in a whole flammability concentration range (4–75 vol.% H_2), namely in ultra-lean, lean, near stoichiometric and rich hydrogen-air mixtures under normal conditions.

2 Experimental setup

The basic idea of a series of the recent our works on flames in horizontal Hele-Shaw cell is to overcome the limitations of the well-established experimental scheme, focused on the spherically expanding 3-dim flames, where only the 2-dim flame surfaces can be studied in details, and it is hardly possible to

Correspondence to: moskalefff@gmail.com

visualize directly he “inner” zones behind the reaction front and, consequently, and to observe, record and differentiate ontogenesis of the flames in hydrogen-air m mixtures with different stoichiometry.

To study the two principal ontogenetic characteristics of the hydrogen-air flame propagation – morphology and dynamics – we used a combination of the visualization of trails of a hydrogen-air flame, which are formed during the condensation of the reaction product (water vapor) on the inner transparent surface of the upper wall of a horizontal Hele-Shaw cell, in reflected visible light and three experimental features that were not used in a systemic way by the other researcher groups: a) horizontal location of the Hele-Shaw cell to minimize the influence of gravity and buoyancy effects; b) closeness of the Hele-Shaw cell to study initially quiescent gas mixture; c) central ignition of the hydrogen-air mixture in a Hele-Shaw cylindrical cell. Figure 1 shows examples of such condensation trails formed in a horizontal cylindrical Hele-Shaw cell during the combustion of hydrogen-air mixtures with different initial hydrogen concentrations.

Figure 1. Condensation trails in a horizontal cylindrical Hele-Shaw cell during the combustion of hydrogen-air mixtures with different initial hydrogen concentrations: left – 10 vol.% H_2; center – 18.1 vol.% H_2; right – 50 vol.% H_2.

Above-described features allowed us to study in detail the 2-dim fronts of the free cylindrically symmetric expansion of ultra-lean quasi-2-dim hydrogen-air flames with different morphologies and dynamics during their development in time. In other word, experiments in horizontal, symmetrical Hele-Shaw cell permit a 2-dim “tomographic” study of the free outward spherically expanding 3-dim flames, thoroughly studied previously.

In this report we used digital video recordings obtained at the National Research Center “Kurchatov Institute” (Russia) in 2019 – 2021 for the following experimental conditions. Combustion of hydrogen-air mixtures was initiated in a horizontal cylindrical Hele-Shaw cell with an inner diameter of 150 mm. The upper and lower bases of the cylindrical chamber were located parallel to each other at a distance of 5 mm, as shown in Figure 2.

Cylindrical side wall and bottom base were made of caprolon sheet. Through a hole in this base, the chamber was connected to the systems for preparing the gas mixture and measuring the static pressure in the chamber. The upper base of the camera was made of transparent flat quartz glass for visual observation and video recording. Before each experiment, the chamber was evacuated to a residual pressure of P_r = 0.025 kPa, after which hydrogen was supplied there to a predetermined pressure P_{H2}, and then atmospheric air with a pressure P_0 = 101.325 kPa and an absolute temperature T_0 = 297 K. Thus, the total pressure of the gas mixture was equal to P_0, and the volume concentration of hydrogen was determined by the pressure ratio $[H_2] = P_{H2}/P_0 = x$ and controlled using laboratory pressure gauges with an accuracy of 0.05 vol.% H_2.

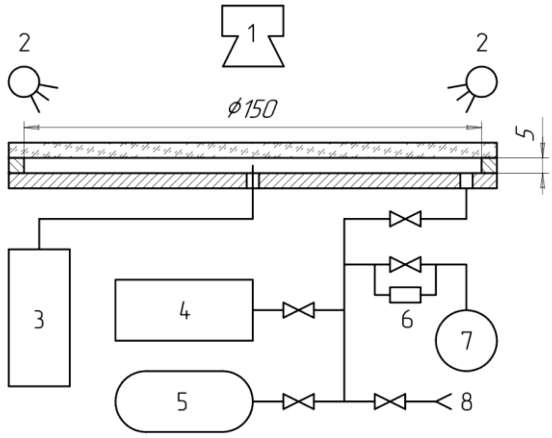

Figure 2. Experimental setup: 1 – video camera; 2 – backlight; 3 – high-voltage generator; 4 – vacuum pump; 5 – cylinder with hydrogen; 6 – differential pressure gauge; 7 – high precision vacuum gauge; 8 – air supply.

Condensation of water vapor after the passage of the hydrogen-air flame front near the upper flat optically transparent wall of the Hele-Shaw cell allowed us to visualize the dynamics of the flame propagation process due to the dispersion of light from an external source on condensed microdroplets. On the one hand, this experimental technique guaranteed the non-invasiveness of our observations, and on the other hand, it fixed the propagation trajectories of ultra-lean hydrogen-air flame fronts with extremely low luminosity in the optical range.

Details of the experimental setup, measurement procedures and video capturing of the flames have been described in [9]. Additional video camera was used – Evercam 2000-8-C, resolution 1280×860 pixels, maximum frame speed 44500 fps, frame speed at max resolution 2000 fps.

3 Flame front trajectories

The time dependencies of the leading points of the flame fronts have been obtained, using the frame-by-frame difference projections. To approximate the dependences $s(t)$, shown at Figure 3, we use an exponential model of the form:

$$s_i = b_0 \cdot (1 - \exp(-b_1 \cdot t_i)) + e_i, \qquad (1)$$

where $b = (b_0, b_1)$ is a parameters vector, estimated by the nonlinear least squares method. The residual standard error for models (1) does not exceed 1 mm over the entire range of hydrogen volume concentrations in air $6.8 \leq x \leq 60$ vol.% H_2, which indicates the adequacy of model (1) to the observed data.

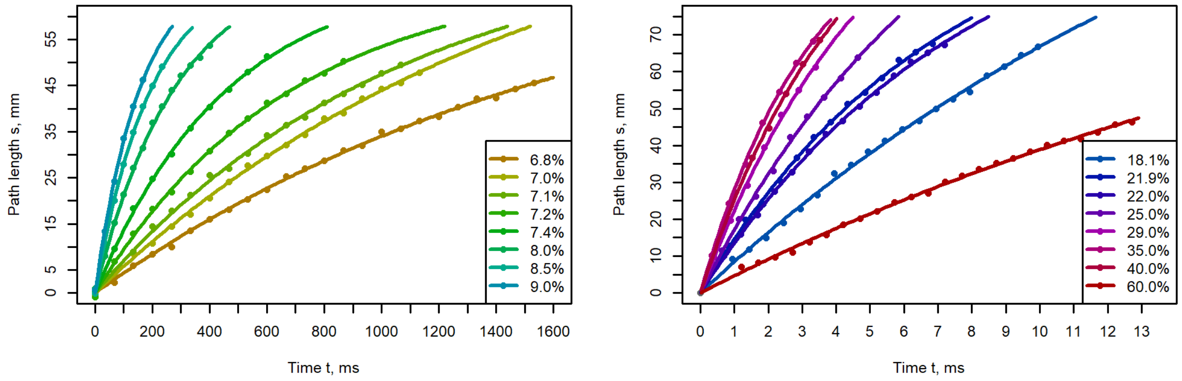

Figure 3. Flame fronts (leading points) positions $s(t)$ vs time t: left – in ultra-lean; right – in lean, near stoichiometric and rich hydrogen-air mixtures under normal conditions.

4 Initial and terminal velocities of flame fronts

As well as for the ultra-lean flames [7], dynamics of the lean, near stoichiometric and rich flames demonstrated similar trend: maximal front velocity was at the beginning and gradual deceleration later.

Differentiation of models (1) obtained at different hydrogen concentrations allows us to find dependences for both initial $v_0(x)$ and terminal $v_1(x)$ flame front propagation velocities shown in Figure 4 by colored triangles up and down:

$$v_0 = b_0 \cdot b_1, \qquad v_1 = (b_0 - s_1) \cdot b_1 \tag{2}$$

where s_1 = 75 mm is the terminal length of the flame front path corresponding to the radius of the horizontal cylindrical Hele-Shaw cell. White triangles with dark gray contours in Figure 4 show the estimates of the initial and terminal velocities made using the model (1)-(2) based on the experimental data published in [8].

To approximate the dependences $v_0(x)$ and $v_1(x)$ shown in Figure 4 by thickened solid dark gray lines, we use a model of the form:

$$v_i = \frac{c_0}{\mathrm{B}(c_1, c_2)} x_{0i}^{b_1 - 1} (1 - x_{0i})^{b_2 - 1} + e_i; \qquad x_{0i} = \frac{x_i - 5.5}{73.5 - 5.5}, \tag{3}$$

where $c = (c_0, c_1, c_2)$ is a parameters vector, estimated by the nonlinear least squares method; x_{0i} is the molar fraction of hydrogen in the air, displayed on the segment [0, 1]; $\mathrm{B}(c_1, c_2)$ is the Euler integral of the first kind. The residual standard error for models (3) does not exceed 1 m/s over the entire range of hydrogen volume concentrations in air $6.8 \le x \le 60$ vol.% H_2, which indicates the adequacy of model (3) to the observed data.

Considering the constructed models (3), we can estimate the hydrogen concentration in the air x_{max} = 36.6 vol.% H_2, corresponding to the highest flame front propagation velocities (initial and terminal) in a horizontal cylindrical Hele-Shaw cell. This concentration is shown in Figure 4 as a vertical dashed gray line.

Drastic changes in flame dynamics were observed in concentration range, where the Flame Ball-to-Deflagration Transition phenomenon [11] takes place.

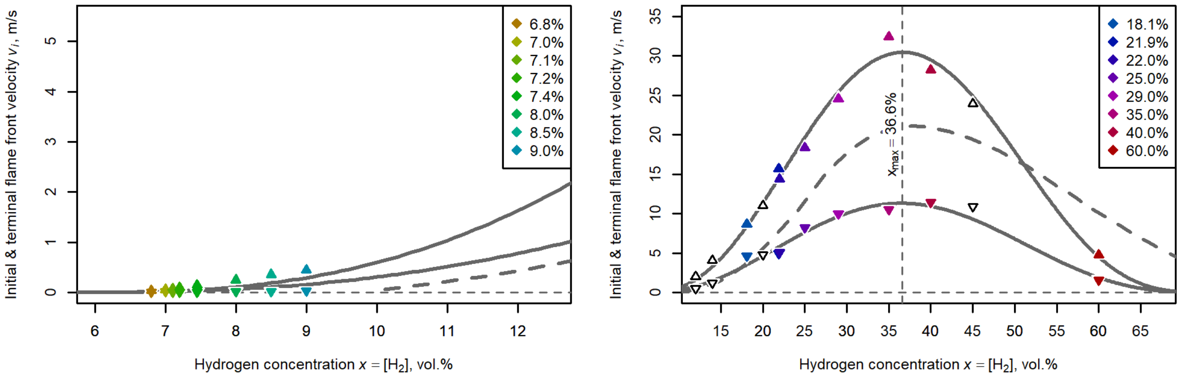

Figure 4. Dependencies for the initial (triangle up) v_0 and terminal (triangle down) v_1 flame front velocities upon the hydrogen volume fraction $x = [H_2]$ in: left –ultra-lean lean, where discrete fronts were recorded, and right – near-stoichiometric and rich mixtures (6.8–60 vol.% H_2), where the continuous fronts were recorded.

At Figure 4 dark gray dashed line represents dependence of burning speed – $v_b = v_L \cdot \sigma$ – of the hydrogen-air deflagration flames upon stoichiometry. Normal laminar flame velocity v_L dependence upon initial hydrogen concentration in mixture was extracted from [10]. Values of expansion ratio $\sigma = \frac{T_{AICC}}{T_u}$ were computed by using Chemical WorkBench program [12].

5 Conclusions

1. Changes in dynamics of the quasi-2-dim cylindrically expanding hydrogen-air flames were systematically studied in horizontal Hele-Shaw cell for a whole flammability range of the quiescent hydrogen-air mixtures under normal initial conditions (pressure and temperature).

2. It was proposed to use a dependence of the flame front position upon time $s(t)$ as an integral characteristic of the flame dynamics. Three specific derivatives of the flame front path – 1) initial and 2) terminal front velocities, and 3) deceleration rates permit to quantitatively characterize the ontogenetic development of the flames in 2-dim case. For 3-dim case an initial acceleration of the flames can be fourth characteristic of flame dynamic too.

3. For all stoichiometries maximal burning velocities of the cylindrically expanding flames were fixed at initial moment with subsequent deceleration.

4. Drastic changes in flame dynamics were observed in concentration range, where the Flame Ball-to-Deflagration Transition (9–10 vol.% H_2) phenomenon takes place.

5. Pulsation of the flame front was observed both in lean and rich mixtures. More detailed study and quantification of this, probably, thermoacoustic effect, previously comprehensively studied for rectangular geometry [13,14], is necessary for the horizontal cylindrical closed Hele-Shaw cells.

References

[1] Dowdy, D.R., Smith, D.B., Taylor, S.C. and Williams, A. (1991) The use of expanding spherical flames to determine burning velocities and stretch effects in hydrogen/air mixtures. Proceedings of the Combustion Institute, 23-1: 325-332.

[2] Kumar, S.R. (1998) Laminar Burning Velocities of Lean Hydrogen-Air Mixtures. EDL Report FM97-15. California Institute of Technology.

[3] Cheikhravat, H., Chaumeix, N., Bentaib, A., Paillard, C.E. (2012) Flammability Limits of Hydrogen-Air Mixtures. Nuclear Technology 178-1: 5-16.

[4] Kim, W.K., Mogi, T., Kuwana, K. and Dobashi, R., (2015) Self-similar propagation of expanding spherical flames in large scale gas explosions, Proc. of the Combustion Institute, 35-2: 2051-2058.

[5] Bauwens, C.R., Bergthorson, J.M. and Dorofeev, S.B. (2015) Experimental study of spherical-flame acceleration mechanisms in large-scale propane–air flames, Proceedings of the Combustion Institute, 35-2: 2059-2066.

[6] Sun, Z.Yu., Li, G.X. (2016) Propagation characteristics of laminar spherical flames within homogeneous hydrogen-air mixtures. Energy. 116-1: 116-127.

[7] Moskalev, P.V., et al. (2022). Scaling Laws for Velocity Dynamics of the Ultra-Lean Hydrogen-Air Flames Expanding in Horizontal Cylindrical Hele-Shaw Cell. 28th ICDERS.

[8] Grune, J., Sempert, K., Kuznetsov, M., Jordan, T., Experimental investigation of unconfined spherical and cylindrical flame propagation in hydrogen-air mixtures. (2021). Int. J. Hydrogen Energy. 46(23): 12487-12496.

[9] Denisenko, VP, et al. (2021). Critical morphological phenomena during ultra-lean hydrogen-air combustion in closed horizontal Hele-Shaw cell. Proc. ICHS-2021. Paper 128.

[10] Pitz, W. J., Westbrook C. K. (2008). Chemical Kinetic Modeling of Hydrogen Combustion Limits, LLNL-TR-402715.

[11] Kirillov, I.A., On Flame Ball-to Deflagration Transition in hydrogen-air mixtures, ICHS2021, paper 134.

[12] Chemical WorkBench – integrated tool for kinetic and thermodynamic calculations: https://www.kintechlab.com/products/chemical-workbench/.

[13] Veiga-Lopez, F., et al. (2019) Experimental analysis of oscillatory premixed flames in a Hele-Shaw cell propagation towards a closed end. Combustion and Flame 201: 1-11.

[14] Kuznetsov, M., et al. (2020). Thermoacoustic analysis of lean premixed hydrogen flames in narrow vertical channels. Fuel 278-15: 118212.